

# Dalton Transactions

Accepted Manuscript



This is an *Accepted Manuscript*, which has been through the Royal Society of Chemistry peer review process and has been accepted for publication.

*Accepted Manuscripts* are published online shortly after acceptance, before technical editing, formatting and proof reading. Using this free service, authors can make their results available to the community, in citable form, before we publish the edited article. We will replace this *Accepted Manuscript* with the edited and formatted *Advance Article* as soon as it is available.

You can find more information about *Accepted Manuscripts* in the [Information for Authors](#).

Please note that technical editing may introduce minor changes to the text and/or graphics, which may alter content. The journal's standard [Terms & Conditions](#) and the [Ethical guidelines](#) still apply. In no event shall the Royal Society of Chemistry be held responsible for any errors or omissions in this *Accepted Manuscript* or any consequences arising from the use of any information it contains.

**Naked-Eye Detections and Thermochromic Properties on the Cu(II)-3,3'-  
thiodipropionate Complexes with Benzimidazole**

**Mürsel Arıcı<sup>a</sup>, Okan Zafer Yeşilel<sup>\*a</sup>, Murat Taş<sup>b</sup>**

<sup>a</sup>Department of Chemistry, Faculty of Arts and Sciences, Eskişehir Osmangazi University,  
26480 Eskişehir, Turkey

<sup>b</sup>Department of Science Education, Education Faculty, Ondokuz Mayıs University, 55139,  
Samsun, Turkey

**Abstract**

Two new coordination compounds having naked-eye sensor properties and thermochromic behaviors, namely,  $[\text{Cu}(\text{tdp})(\text{H}_2\text{O})(\text{bim})_3] \cdot 4\text{H}_2\text{O}$  (**1**) and  $\{[\text{Cu}(\mu_2\text{-tdp})(\text{bim})_2] \cdot 4\text{H}_2\text{O}\}_n$  (**2**) (tdp = 3,3'-thiodipropionate, bim = benzimidazole) were synthesized and structurally characterized by elemental analysis, IR and UV spectra, and single-crystal X-ray diffraction, powder X-ray diffraction (PXRD) and thermal analyses (TG, DTA and DTG) techniques. Complex **1** changed the color from blue to dark and light green in methanol and DMF solvents, respectively, while complex **2** changed the color from light blue to light green in only DMF solvent. Moreover, complex **1** can detect the methanol in ethanol up to 10 percent through the naked-eye. Thermochromic properties of the complexes showed that complexes **1** and **2** changed the color from blue and light blue to dark green at 65°C, respectively.

**Keywords:** 3,3'-thiodipropionate complexes; Thermochromic behavior; naked-eye detection.

**\*Corresponding Author:**

E-mail: yesilel@ogu.edu.tr

Tel: +902222393750, Fax: +902222393578

## 1. Introduction

The studies related to chromotropism (color change of material depending on chemical or physical conditions) behaviors of coordination complexes have received considerable attention because of their potential applications such as molecular-switching, color indicator, optic sensor, thermo-sensor and chemical sensor<sup>1-7</sup>. In the coordination complexes, color change of material can occur as a result of interaction of solvent and compound or changing of coordination geometry around the metal center<sup>3, 4, 6</sup>. Therefore, the studies with respect to determination of the reason of color change are important. In recent years, solvatochromic properties of coordination complexes have also been investigated to utilize as a chemosensor<sup>2</sup>. There have been intensive researches on chemosensor for specific or selective detections of analytes<sup>8-11</sup>. Especially, chemosensor studies related to selective solvent detections like methanol, ethanol etc. have been paid attention due to the fact that these solvents have been widely used in many fields<sup>8, 12-14</sup>. Although methanol is toxic and poisonousness for human body, sometimes, methanol is mixed into ethanol in imitation *Turkish Raki* or wine to reduce the cost of ethanol<sup>12, 13</sup>. This situation can give rise to headache, vomiting, blindness even death<sup>13</sup>. Therefore, the rapid detection of methanol in ethanol is very important. In the literature, there are many instrumental methods such as luminescence spectroscopy, high performance liquid chromatography, GC/MS etc. for the detection of methanol in ethanol<sup>12, 13, 15, 16</sup>. However, these are very expensive instruments and not practical in daily life. Hence, the development of specific or selective colorimetric sensors for rapid detection of methanol in ethanol is very important. Generally, coordination complexes (or coordination polymers) are utilized for colorimetric sensor studies<sup>8</sup>.

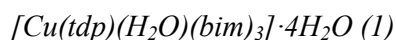
In this study, two mixed-ligand copper(II) complexes were synthesized using  $\text{Cu}(\text{CH}_3\text{COO})_2 \cdot \text{H}_2\text{O}$ , 3,3'-thiodipropionic acid and benzimidazole ligands. 3,3'-thiodipropionic acid ( $\text{tdpH}_2$ ) was an aliphatic dicarboxylic acid with five potential donor atoms (four of which come from two carboxylate groups and one of which come from

thioether group) was used in the syntheses of supramolecular coordination polymers<sup>17, 18</sup>. These complexes were characterized by elemental analysis, IR and UV spectra, thermogravimetric (TG, DTA) and X-ray diffraction techniques. Moreover, solvent sensing properties and thermochromic behaviors of the complexes were investigated.

## 2. Materials and Physical measurements

All chemicals were commercially available and were used without further purification. Elemental analyses (C, H, and N) were performed on a Perkin-Elmer 2400C Elemental Analyzer. IR spectra were recorded on a Bruker Tensor 27 FT-IR spectrometer using KBr pellets in the range 400–4000 cm<sup>-1</sup>. UV-vis spectra were recorded on a Perkin Elmer Lambda 35 spectrometer in 10<sup>-3</sup> M solution. Thermal analyses (TGA, DTG and DTA) were carried out with a Perkin Elmer Diamond TG/DTA Thermal Analyzer in the static air atmosphere with a heating rate of 10 °C/min in the temperature range 30–800 °C. Powder X-ray diffraction patterns (PXRD) were obtained from 5 to 50° 2θ at a rate of 5°/min using a Rikagu Smartlab X-ray diffractometer operating at 40 kV and 30 mA with Cu-Kα radiation (λ= 1.5406 nm). Diffraction measurements for **1** and **2** were carried out on Agilent Diffraction SuperNova and Bruker APEX-II CCD diffractometers that were equipped with MoKα (0.71073 Å) radiation at 293 K. The structures were solved by direct methods using OLEX2<sup>19</sup> and SHELXS<sup>20</sup>, with anisotropic thermal parameters for all non-hydrogen atoms. All non-hydrogen atoms were refined anisotropically by full-matrix least squares methods<sup>20</sup>. Molecular drawings were obtained using Mercury<sup>21</sup>.

### 2.1 Syntheses of the complexes



A mixture of Cu(CH<sub>3</sub>COO)<sub>2</sub>·H<sub>2</sub>O (1 mmol, 0.200 g) and 3,3'-thiodipropionic acid (tdpH<sub>2</sub>) (1 mmol, 0.178 g) in water (20 mL) was stirred at 70°C for 30 minutes and then benzimidazole (2 mmol, 0.244 g) in the mixture of ethanol:DMF (10:1v:v) (20 ml) was added into the mixture. The clear solution obtained was stirred at 70°C for an hour. Resulting

solution was filtered and evaporated at room temperature. The blue crystals were obtained after one week. Yield: 0.286 g, 44.14 % based on  $\text{Cu}(\text{CH}_3\text{COO})_2 \cdot \text{H}_2\text{O}$ . Anal. Calcd. for  $\text{C}_{27}\text{H}_{36}\text{N}_6\text{O}_9\text{SCu}$ : C, 47.40; H, 5.30; N, 12.28; S, 4.69 %. Found: C, 47.70; H, 5.19; N, 12.20; S, 4.33 %. IR (KBr,  $\text{cm}^{-1}$ ): 3377 (br), 3140, 3113 (w), 2976 (w), 2912 (w), 1587 (vs), 1495 (m), 1423 (m), 1387(m), 846 (w), 746 (vs)  $\text{cm}^{-1}$ .



The synthetic procedure for **2** is similar to that for **1**. However, only the mixture of water (20 mL) and ethanol (20 mL) was used in the synthesis of **2**. The light blue crystals of **2** were obtained after five days. Yield: 0.194 g, 71 % (based on  $\text{Cu}(\text{CH}_3\text{COO})_2 \cdot \text{H}_2\text{O}$ ). Anal. Calcd. for  $\text{C}_{20}\text{H}_{28}\text{N}_4\text{O}_8\text{SCu}$ : C, 43.83; H, 5.15; N, 10.22; S, 5.85 %. Found: C, 44.02; H, 5.09; N, 10.87; S, 5.32 %. IR (KBr,  $\text{cm}^{-1}$ ): 3414 (br), 3315 (w), 3105 (m), 3055 (w) 2989 (w), 2920 (w), 1562 (vs), 1504 (w), 1433 (vs), 1304 (s), 847 (w), 746 (s)  $\text{cm}^{-1}$ .

### 3. Results and Discussion

#### 3.1 Synthesis and Characterization

Complexes **1** and **2** were obtained by reaction of  $\text{Cu}(\text{CH}_3\text{COO})_2 \cdot \text{H}_2\text{O}$ , 3,3'-thiodipropionic acid and benzimidazole ligand. Only solvents were changed in the reaction medium. When the mixture of water:ethanol:DMF as solvent was used in the reaction, mononuclear copper(II) complex (**1**) was obtained. In the mixture of water:ethanol, one dimensional (1D) coordination polymer (**2**) was obtained. As a result, solvent is an important factor on the structure in the reaction medium. Synthesized complexes were characterized by elemental analysis, IR spectra and single crystal X-ray diffraction technique. Elemental analysis results are consistent with the assigned formulations. In the IR spectra of complexes **1** and **2**, broad bands observed at 3377 and 3414  $\text{cm}^{-1}$  are due to  $\nu(\text{O-H})$  stretching vibrations of water molecules, respectively. The bands observed between at 3315 and 3105  $\text{cm}^{-1}$  are attributed to the  $\nu(\text{N-H})$  stretching vibrations of benzimidazole ligand. For **1** and **2**, the absorption bands appearing between at 3113 and 3055  $\text{cm}^{-1}$  are due to aromatic  $\nu(\text{C-H})$

stretching. Aliphatic  $\nu(\text{C-H})$  stretching vibrations for **1** and **2** are observed in the range of 2989-2912  $\text{cm}^{-1}$ . The asymmetric and symmetric stretching vibrations corresponding to carboxylate groups of  $\text{tdpH}_2$  are observed at 1695 and 1429  $\text{cm}^{-1}$ , respectively. The strong asymmetric vibration at 1695  $\text{cm}^{-1}$  of  $\text{tdpH}_2$  was disappeared after conversion to complexes **1** and **2**. This indicates the full deprotonation of carboxylate groups of  $\text{tdpH}_2$ , as seen by single crystal results. For **1** and **2**, the asymmetric vibrations are observed at 1587 and 1562  $\text{cm}^{-1}$ , respectively. The bands at 1387 and 1433  $\text{cm}^{-1}$  are due to the symmetric stretching vibrations of carboxylate groups, respectively. The characteristic thioether ( $\text{C-S-C}$ ) stretching vibrations of complexes **1** and **2** are observed between at 847 and 746  $\text{cm}^{-1}$ .

### 3.2 Description of structures

The crystal data and the refinement details of complexes are given in Table 1. Selected bond distances and angles and hydrogen bonding geometry are listed in Table S1 and Table S2, respectively.

#### *[Cu(tdp)(H<sub>2</sub>O)(bim)<sub>3</sub>]·4H<sub>2</sub>O (1)*

The crystal structure of **1** with atom numbering scheme is shown in Fig. 1. The selected bond lengths, bond angles and hydrogen bonding geometry are given in Table S1. The complex crystallizes in monoclinic system and  $\text{C2/c}$  space group. The asymmetric unit of **1** contains a  $\text{Cu(II)}$  ion, one  $\text{tdp}$ , three  $\text{bim}$  and one aqua ligands and four crystal water molecules, as seen in Fig. 1. The  $\text{Cu(II)}$  ion is coordinated by three nitrogen atoms from three different  $\text{bim}$  ligands, one carboxylate oxygen atom from  $\text{tdp}$  ligand and one aqua ligand, forming a distorted square pyramidal geometry (The value of  $\tau$  is 0.13)<sup>22</sup>.  $\text{Tdp}$  ion binds to  $\text{Cu(II)}$  ion through the carboxylate oxygen atom as a monodentate ligand. To the best of our knowledge, this coordination mode of  $\text{tdp}$  ligand is observed for the first time in complex **1**.

The crystal packing of **1** is stabilized through strong intra- and intermolecular hydrogen bonding,  $\text{C-H}\cdots\pi$  and  $\pi\cdots\pi$  interactions (Fig. S1 and Fig. 2 (a)). One dimensional chain (1D) generates via  $\text{C-H}\cdots\pi$  interaction between the  $\text{C7-H7}$ ,  $\text{C19-H19}$  and benzene rings

(Cg1 : C22-C23-C24-C25-C26-C27, Cg2 = C8-C9-C10-C11-C12-C13; C7 $\cdots$ Cg1<sup>i</sup> = 3.42(1) Å and C19 $\cdots$ Cg2<sup>ii</sup> = 3.65(1) Å (i): x, -1+y, z; (ii) x,-y, ½+z] and hydrogen bonding between N-H group of benzimidazole ligand and oxygen atom of carboxyl group of tdp ligand [N2 $\cdots$ O2<sup>i</sup> = 2.826 Å, H2 $\cdots$ O2<sup>i</sup> = 2.017 Å and N2-H2 $\cdots$ O2<sup>i</sup> = 156.53 °, (i) = x, -1+y, z] (Fig. S1 (a)). The 1D supramolecular chains are further linked by O-H $\cdots$ O hydrogen bonding interactions to form a 2D supramolecular network (Fig. 2 (a)). The most striking feature of the complex is the existence of D3 type water cluster [O7 $\cdots$ O8 = 2.86(1) ve O8 $\cdots$ O9 = 2.82(1) Å]. These clusters are connected to the coordinated water molecule (O5) and other crystal water molecule (O6) to generate five member water clusters (Fig. 2 (b)). Strong hydrogen bonds between crystal water molecules having D3 type motifs and uncoordinated oxygen atoms of carboxyl group of tdp are also important for the formation of 2D supramolecular network. These 2D structures extend into a 3D supramolecular network by  $\pi\cdots\pi$  interactions between the benzene rings (Cg2) (Cg2 $\cdots$ Cg2<sup>i</sup> = 3.937(6) Å, (i): ½-x,-½-y, 1-z) (Fig. S1 (d)).

### **$\{[Cu(\mu_2\text{-tdp})(bim)_2]\cdot 4H_2O\}_n$ (2)**

Although the complex **2** contains the same components with complex **1**, the complex **2** was obtained into the different solvent medium. In the complex **1**, the mixture of water:ethanol as solvent was used to instead of water:ethanol:DMF in the complex **2**. In **2**, tdp ligand coordinated to the Cu(II) ion with different coordination mode.

The molecular structure of **2** with the atom labeling is shown in Fig. 3. The X-ray crystal structure analysis reveals that complex crystallizes in the monoclinic system, C2/c space group. The molecular structure of **2** contains one Cu(II) ion, one tdp and two bim ligands and four crystal water molecules (Fig. 3). Each Cu(II) center is coordinated by four oxygen (O1, O2, O1<sup>i</sup> and O2<sup>i</sup> (i) -x, y, 1.5-z) and two nitrogen atoms (N1 and N1<sup>i</sup>) from two bim ligands, to give a distorted octahedral geometry. Two Cu(II) ions are bridged by tdp ligand via four carboxylate oxygen atoms to form 1D coordination polymer and Cu1-Cu1<sup>i</sup>

distance is 10.153 Å (Fig. 4). The adjacent chains are further linked together by  $\pi\cdots\pi$  interactions between benzimidazole ligands to form a two-dimensional (2D) network (Cg1 = N1-C4-N2-C5-C10, Cg2 = C5-C6-C7-C8-C9-C10,  $Cg1\cdots Cg2^i = 3.545(3)$ , (i) -x, -y, 2-z) (Fig. 4). The adjacent layers extend into a 3D supramolecular network by N-H $\cdots$ O and O-H $\cdots$ O hydrogen bonds and C-H $\cdots\pi$  interactions between C3-H3A and benzene ring ( $C3\cdots Cg2 = 3.609(6)$  Å and  $C3-H3A\cdots Cg2 = 132^\circ$ ) (Fig. S2). The 3D supramolecular network contains 1D channel that is filled with crystal water molecules having D2 form (Fig. 5).

### 3.3 Solvent Sensing Properties

Solvatochromic properties of the complexes are very important for applications such as color indicator and chemical sensor, etc. In this study, dichloromethane (DCM), ethanol (EtOH), methanol (MetOH), dimethylformamide (DMF) solvents were used to determine solvent sensing properties of the complexes. These solvents were exposed to complexes **1** and **2**. Complexes **1** changed the color from blue to dark and light green in only methanol and DMF solvents (Fig. 6). UV-vis spectra of compounds **1** and **2** were measured to show color changes in MetOH and DMF. UV-vis spectra of complex **1** in MetOH and DMF showed that wavelength of complex **1** shifted to visible region, indicating color changes (Fig. S3). Moreover, thermal analysis curves, PXRD patterns and IR spectra of complex **1** were recorded after exposed to methanol and DMF to determine the reason of color change. Thermal analysis curves of **1** and **1@DMF** or **1@MetOH** are given in Fig. 7a. As seen in Fig. 7a, **1@DMF** does not contain any solvent molecules and is stable up to 103 °C when compared to that of as-synthesized complex **1**. The color change of **1@DMF** can be due to geometry change. This situation indicates a change in coordination environment from distorted square pyramidal to square planar or tetrahedral. TG curve of **1@MetOH** shows that the weight loss in temperature range 38-106°C corresponds to removal of three water molecules (found: 8.82 %; calcd.:8.33 %). Therefore, **1@MetOH** has still water molecules in



the structure. PXRD patterns show that small shifts in some diffraction peaks of **1**@MetOH and **1**@DMF according to as-synthesized complex can be due to geometry change (Fig. S5). IR spectrum of **1**@MetOH shows the existence of water molecules in the structure (Fig. 7b). IR spectra show that asymmetric stretching vibrations of tdp ligand in **1**@DMF or **1**@MetOH shift lower frequency according to as-synthesized complex **1**. Broad band which is due to  $\nu(\text{O-H})$  stretching vibrations of water molecule shifts higher frequency. Because, hydrogen bonds between water molecules or water molecule and benzimidazole ligand will decreased and  $\nu(\text{O-H})$  stretching vibrations will shift higher frequency when complex **1** interacts with MetOH or DMF (Fig. 7b). Hence, complex **1** changes the color in DMF or methanol. The color change property of complex **1** was also studied in C1-C4 alcohols. Interestingly, complex **1** has unique response to methanol among the other alcohols. Moreover, the color change of complex **1** was investigated in the mixture of methanol:ethanol. As known, the detection of methanol in ethanol has been very important because of its toxic and poisonousness for human. In the literature, the study with respect to naked-eyed detection of methanol is very rare <sup>8, 14</sup>. Complex **1** changed the color in the mixture (10:1, v:v) of ethanol:methanol about at 5 min. As seen in Fig. S1, there are water molecules in the pores of supramolecular structure of **1**. The color change of complex **1** in methanol may be due to the fact that small molecule methanol is easily exchanged with water molecules in the pores. The easy interaction of methanol with complex **1** can lead to a change in the ligand-field splitting of Cu(II) ion resulting in color change. This complex can serve as a naked-eye sensor for methanol.

Moreover, complex **2** only changed rapidly the color from light blue to light green in only DMF solvent (Fig. 8). Crystallinity of complex **2** was lost after exposed to DMF. UV-vis spectrum demonstrates the color change due to the fact that absorbance of complex **2** shifts to higher wavelengths (Fig. S4). PXRD pattern of complex **2**@DMF indicated that the positions of the diffraction peaks of complex **2**@DMF are good agreement with those of as-synthesized

complex (Fig. S5). This result shows that the coordination environment of Cu(II) center remains unchanged. Thermal analysis curve and IR spectrum of complex **2** were recorded after exposed to DMF (Fig. 9). TG curve of **2**@DMF demonstrates that lattice water molecules of complex **2** are removed from the structure in the presence of DMF. Furthermore, IR spectrum of **2**@DMF which shows the losses of water molecules is well-matched with TG result. The color change of complex **2** may be attributed to host-guest interaction. This complex can be used for DMF detection.

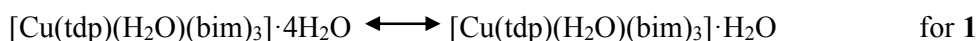
### 3.4 Thermal and Thermochromic Properties

The thermal stabilities and thermal decomposition behaviors of the complexes were employed by thermal analysis in a static air atmosphere in the temperature range 30-800°C, as shown in Figs. 10 and 11. The initial losses occurring from 38-93°C for **1** and 39-137°C for **2** are due to the elimination of five and four H<sub>2</sub>O molecules, respectively. (For **1**, found: 13.68 %; calcd.: 13.88 %, for **2**, found: 12.88 %; calcd.: 13.14 %). After the dehydration steps, complexes **1** and **2** are stable up 161 and 170 °C, respectively. The following weight losses of 73.1 % in the temperature range 161-723°C for **1** and 73.1 % in the temperature range 170-772°C for **2** are attributed to decomposition of three bim and one tdp ligands and two bim and one tdp ligands with endothermic and exothermic picks, respectively. The final residual products of complexes **1** and **2** with weight losses of 11.67 % for **1** and 13.78 % for **2** are possibly CuO (calcd. 12.26 % for **1** and 14.47 % for **2**).

The PXRD patterns of the as-synthesized complexes are well-matched with simulated patterns from their single-crystal structures to check the phase purities of the complexes (Fig. 12).

Solid-state thermochromic complexes are important due to their application areas such as temperature sensors. Thermochromic behaviors of the complexes were investigated at solid state. Complexes **1** and **2** changed the color from blue and light blue to green, respectively after heating at 65 °C. After heating at 65 °C, thermal analysis curves and IR spectra were

recorded again to determine thermochromic mechanisms of the complexes (Figs. 10 and 11). As seen in Figs. 10b and 11b, broad bands observed at 3368 for complex **1** and 3448  $\text{cm}^{-1}$  for complex **2** shrank due to the losses of water molecules after heating at 65°C. As a result of removal of water molecules in the complexes, hydrogen bonds in the structure will decreased and  $\nu(\text{O-H})$  stretching vibrations will shift higher frequency. Therefore, the color changes of the complexes are observed. Thermal analysis curves demonstrate that the initial losses occurring from 38-93°C for **1** and 39-137°C for **2** were due to the eliminations of one and one  $\text{H}_2\text{O}$  molecules, respectively (For **1**, found: 2.93 %; calcd.: 2.78 %, for **2**, found: 2.50 %; calcd.: 3.28 % ) (Figs. 10a and 11a). These results indicate that both complexes contain one water molecule after heating at 65 °C, respectively. Suggested mechanisms for thermochromic behaviors of complexes **1** and **2** correspond to removal of lattice water molecules. Temperature sensitive equilibrium for complexes **1** and **2** can be given at below.



After heating, complexes **1** and **2** were exposure to the moisture. Complexes **1** and **2** returned to blue and light blue with exposure to moisture, respectively (Fig. 12). The PXRD patterns of the as-synthesized, heating and rehydration phase of complexes **1** and **2** were given in Fig. 12. As seen in Fig. 12, the positions of the diffraction peaks of **1**@moisture and **2**@moisture are well-matched with those of as-synthesized complexes. These results demonstrate that heated complexes **1** and **2** gain previous crystal structures after exposure to the moisture and the thermochromic processes of complexes **1** and **2** are reversible. Moreover, IR spectra and TG curves of complexes **1** and **2** were recorded after exposure to moisture. The results showed that IR spectra and TG curves of complex **1** and **2** after exposure to moisture were the same with those of as-synthesized complexes **1** and **2**. Thermochromic behaviors are based on the processes of dehydration and rehydration and thermochromic processes are reversible for complexes **1** and **2**.

## Conclusions

In this study, two new complexes were synthesized and characterized. Solvent sensing and thermochromic properties of complexes were investigated. Complex **1** changed the color in methanol and DMF among the other solvents. Moreover, complex **1** can detect the methanol in ethanol through naked eye. Complex **1** can be a candidate for methanol detector. Complex **2** which only changes the color in DMF can be used as a DMF sensor. Complexes **1** and **2** show reversible thermochromic behaviors at 65 °C which may be used as a thermal sensor.

## Acknowledgments

This work was supported by the *Scientific* Research Fund of Eskişehir Osmangazi University. Project number: 201219A101.

## Supporting Information

Crystallographic data for the structural analysis have been deposited with the Cambridge Crystallographic Data Centre, CCDC No. 1012378 and 1012379 for **1** and **2**, respectively. Copies of this information may be obtained free of charge from the Director, CCDC, 12 Union Road, Cambridge CB2 1EZ, UK (fax: +44-1223-336033; e-mail: [deposit@ccdc.cam.ac.uk](mailto:deposit@ccdc.cam.ac.uk) or www: <http://www.ccdc.cam.ac.uk>)

## References

1. H. Golchoubian, E. Rezaee, G. Bruno and H. A. Rudbari, *Inorg. Chim. Acta*, 2011, **366**, 290-297.
2. L. E. Kreno, K. Leong, O. K. Farha, M. Allendorf, R. P. Van Duyne and J. T. Hupp, *Chem. Rev.*, 2012, **112**, 1105-1125.
3. H. Golchoubian and E. Rezaee, *Polyhedron*, 2013, **55**, 162-168.
4. R. Horikoshi, Y. Funasako, T. Yajima, T. Mochida, Y. Kobayashi and H. Kageyama, *Polyhedron*, 2013, **50**, 66-74.
5. W. Linert, Y. Fukuda and A. Camard, *Coord. Chem. Rev.*, 2001, **218**, 113-152.
6. Z.-Z. Lu, R. Zhang, Y.-Z. Li, Z.-J. Guo and H.-G. Zheng, *J. Am. Chem. Soc.*, 2011, **133**, 4172-4174.
7. C. Shen, T. Sheng, Q. Zhu, S. Hu and X. Wu, *Crystengcomm*, 2012, **14**, 3189-3198.
8. A. D. Naik, K. Robeyns, C. F. Meunier, A. F. Leonard, A. Rotaru, B. Tinant, Y. Filinchuk, B. L. Su and Y. Garcia, *Inorg. Chem.*, 2014, **53**, 1263-1265.
9. Y. W. Choi, G. R. You, M. M. Lee, J. Kim, K.-D. Jung and C. Kim, *Inorg. Chem. Commun.*, 2014, **46**, 43-46.
10. Y. Rachuri, K. K. Bisht and E. Suresh, *Cryst. Growth Des.*, 2014, **14**(7), 3300-3308.
11. H. Khajehsharifi and A. Sheini, *Sensor Actuat. B-Chem.*, 2014, **199**, 457-462.
12. H.-M. Wang, H.-P. Liu, T.-S. Chu, Y.-Y. Yang, Y.-S. Hu, W.-T. Liu and S. W. Ng, *RSC Adv.*, 2014, **4**, 14035-14041.
13. Z. Jin, H. He, H. Zhao, T. Borjigin, F. Sun, D. Zhang and G. Zhu, *Dalton Trans.*, 2013, **42**, 13335-13338.
14. Z. Li, X. Liu, W. Zhao, S. Wang, W. Zhou, L. Wei and M. Yu, *Anal. Chem.*, 2014, **86**, 2521-2525.
15. O. Adeyolu, E. I. Iwuoha, M. R. Smyth and D. Leech, *Analyst*, 1996, **121**, 1885-1889.

16. X. Xu, J. Fillos, K. Ramalingam and A. Rosenthal, *Anal. Methods*, 2012, **4**, 3688-3694.
17. M. Arici, O. Z. Yesilel, O. Sahin and M. Tas, *Polyhedron*, 2014, **71**, 62-68.
18. M. Arici, O. Z. Yesilel, S. Keskin, O. Sahin and O. Buyukgungor, *J. Coord. Chem.*, 2013, **66**, 4093-4106.
19. O. V. Dolomanov, L. J. Bourhis, R. J. Gildea, J. A. K. Howard and H. Puschmann, *J. Appl. Crystallogr.*, 2009, **42**, 339-341.
20. G. M. Sheldrick, *Acta Crystallogr., Sect. A: Found. Crystallogr.*, 2007, **64**, 112-122.
21. C. F. Macrae, P. R. Edgington, P. McCabe, E. Pidcock, G. P. Shields, R. Taylor, M. Towler and J. van De Streek, *J. Appl. Crystallogr.*, 2006, **39**, 453-457.
22. A. W. Addison, T. N. Rao, J. Reedijk, J. Vanriijn and G. C. Verschoor, *J. Chem. Soc.-Dalton Trans.*, 1984, 1349-1356.

**Figure and Table Captions**

**Fig. 1.** View of the asymmetric unit of **1** with atom-labeling scheme

**Fig. 2. (a)** 2D supramolecular network of **1** **(b)** five member water cluster for **1**

**Fig. 3.** View of the asymmetric unit of **2** with atom-labeling scheme

**Fig. 4.** The  $\pi\cdots\pi$  interactions for **2**

**Fig. 5.** 3D supramolecular network of **2** which has D2 water cluster inside the voids

**Fig. 6.** The color change photographs of complex **1** in methanol, ethanol, dichloromethane, dimethylformamide

**Fig. 7.** TG curves (a) and IR spectra (b) of complex **1**, **1@MetOH** and **1@DMF**.

**Fig. 8.** The color change photographs of complex **2** in methanol, ethanol, dichloromethane, dimethylformamide

**Fig. 9.** TG curves and IR spectra of complex **2** and **2@DMF**

**Fig. 10.** TG curves and IR spectra of (a) as-synthesized complex **1** (b) complex **1** after heating at 65°C

**Fig. 11.** TG curves and IR spectra of (a) as-synthesized complex **2** (b) complex **2** after heating at 65°C

**Fig. 12.** The pictures of complexes **1** **(a)** and **2** **(b)** showing color changes based on dehydration and rehydration

**Fig. S1. (a)** The hydrogen bonding interactions and **(b)** the C-H $\cdots\pi$  interactions (c) 3D supramolecular network (d) the  $\pi\cdots\pi$  interactions for **1**

**Fig. S2. (a)** The hydrogen bonding interactions and **(b)** the C-H $\cdots\pi$  interactions for **2**

**Fig. S3.** UV-Vis spectra of complex **1** in water, MetOH and DMF solutions.

**Fig. S4.** UV-Vis spectra of complex **2** in water and DMF solutions.

**Table 1.** Crystal data and structure refinement parameters for complexes **1** and **2**

**Table S1.** Selected bond distances and angles for complexes **1** and **2** (Å, °)

**Table S2.** Hydrogen–bond parameters for complexes **1** and **2** (Å, °)



**Table 1.** Crystal data and structure refinement parameters for complexes **1** and **2**

Crystal data	<b>1</b>	<b>2</b>
Empirical formula	C <sub>27</sub> H <sub>36</sub> CuN <sub>6</sub> O <sub>9</sub> S	C <sub>20</sub> H <sub>28</sub> CuN <sub>4</sub> O <sub>8</sub> S
Formula weight	684.22	548.06
Crystal system	Monoclinic	Monoclinic
Space group	<i>C2/c</i>	<i>C2/c</i>
<i>a</i> (Å)	37.162 (5)	10.1535(5)
<i>b</i> (Å)	8.603 (5)	16.3971(7)
<i>c</i> (Å)	20.236 (5)	15.7138(7)
$\alpha$ (°)	90.00	90.00
$\beta$ (°)	100.733 (5)	106.707(2)
$\gamma$ (°)	90.00	90.00
<i>V</i> (Å <sup>3</sup> )	6356 (4)	2505.7(2)
<i>Z</i>	8	4
<i>D<sub>c</sub></i> (g cm <sup>-3</sup> )	1.430	1.453
$\mu$ (mm <sup>-1</sup> )	0.81	1.00
$\theta$ range (°)	3.2–30.4	5.4–42.8
Measured refls.	13498	4266
Independent refls.	6490	1891
<i>R</i> <sub>int</sub>	0.144	0.051
<i>S</i>	1.02	1.09
<i>R</i> <sub>1</sub> / <i>wR</i> <sub>2</sub>	0.095/0.242	0.056/0.118
$\Delta\rho_{\max}/\Delta\rho_{\min}$ (eÅ <sup>-3</sup> )	1.11/-0.59	0.44/-0.46

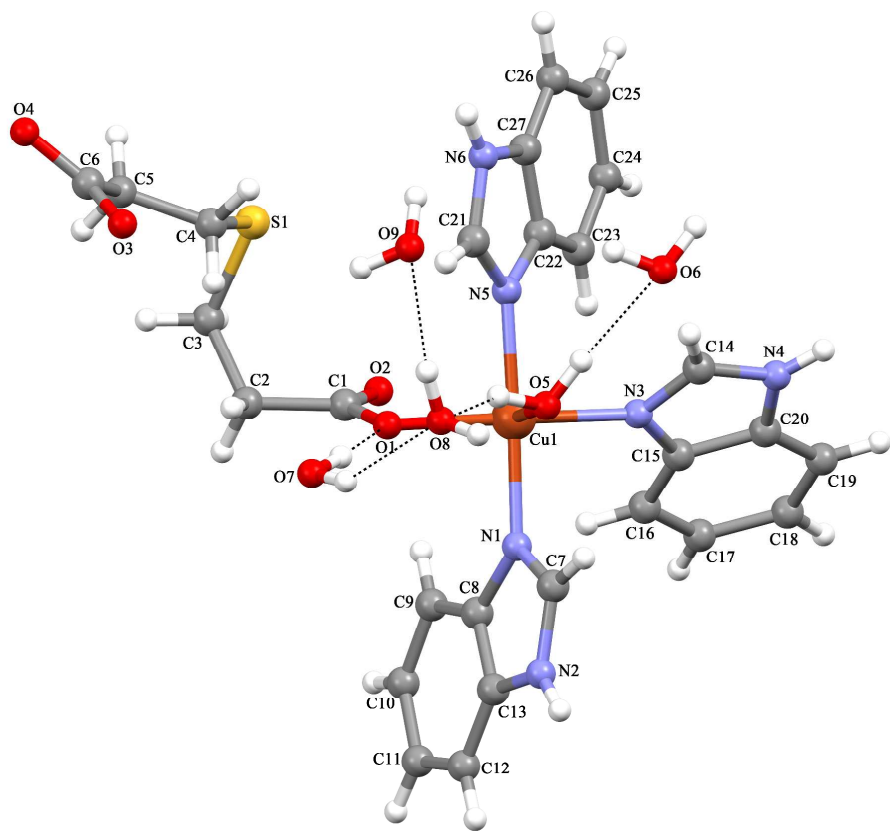


**Fig. 1.** View of the asymmetric unit of 1 with atom-labeling scheme

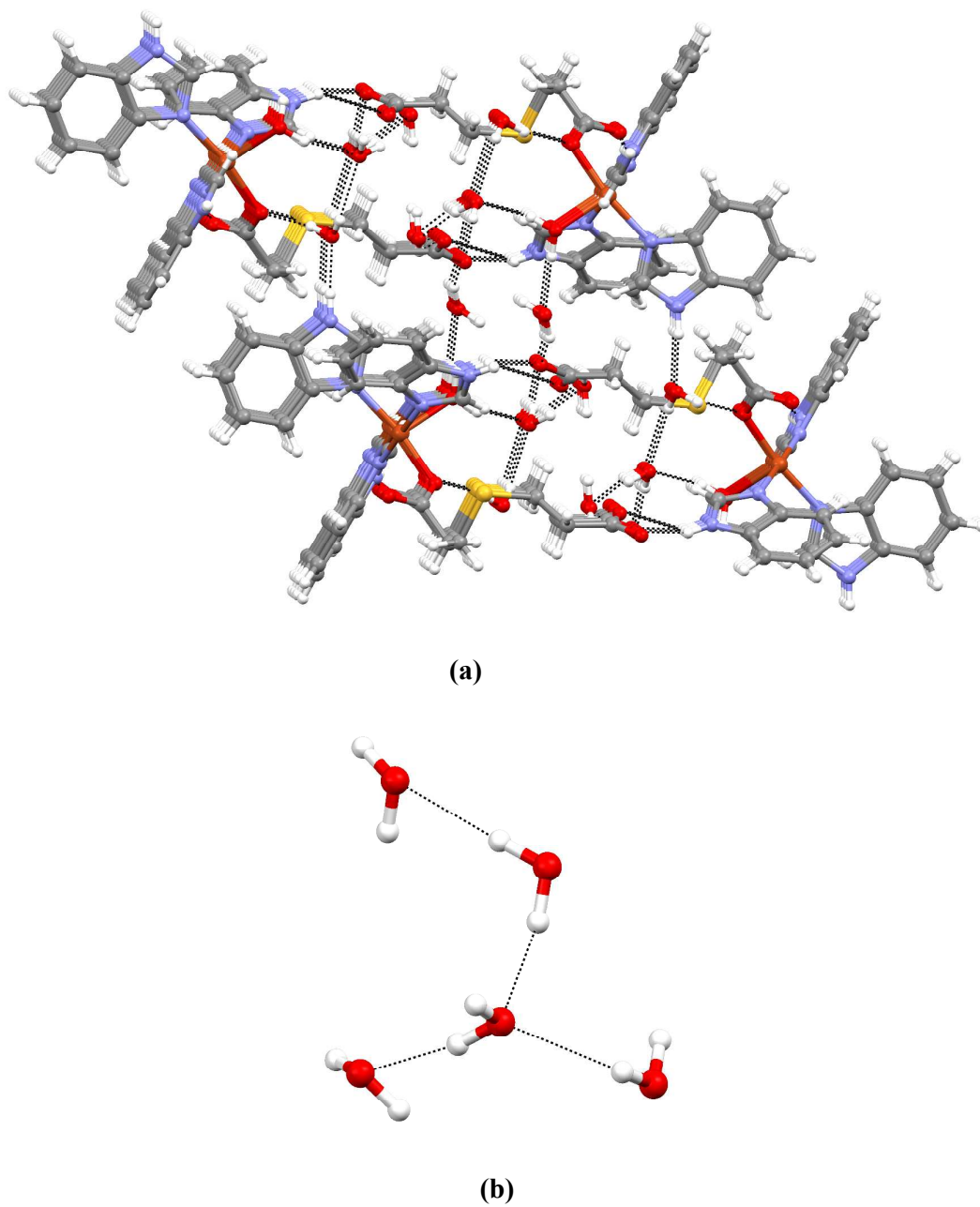


**Fig. 2.** (a) 2D supramolecular network of 1 (b) five member water cluster for 1

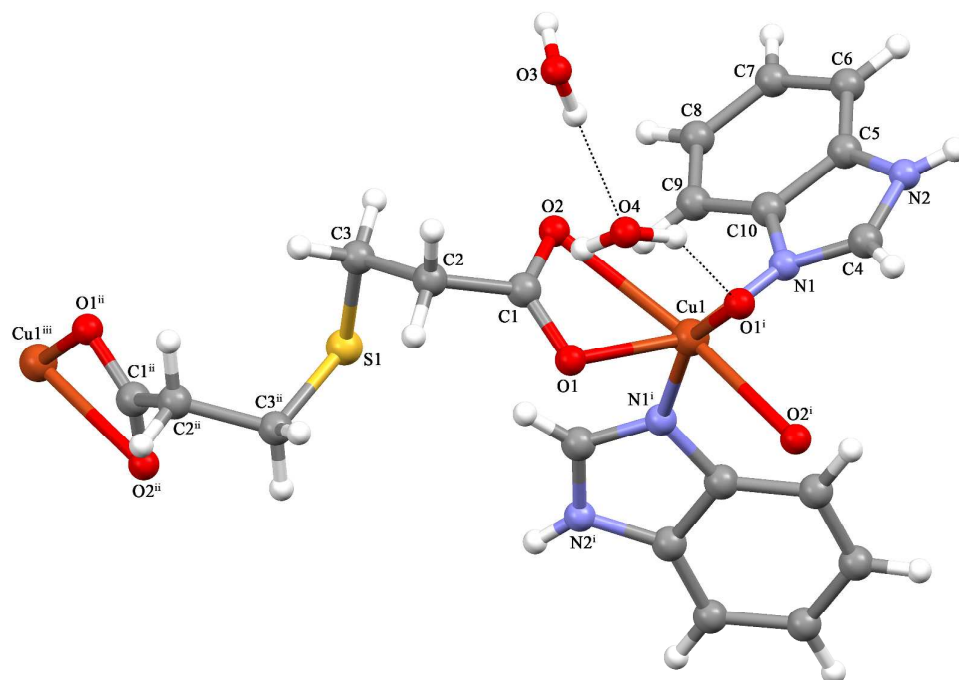


**Fig. 3.** View of the asymmetric unit of **2** with atom-labeling scheme

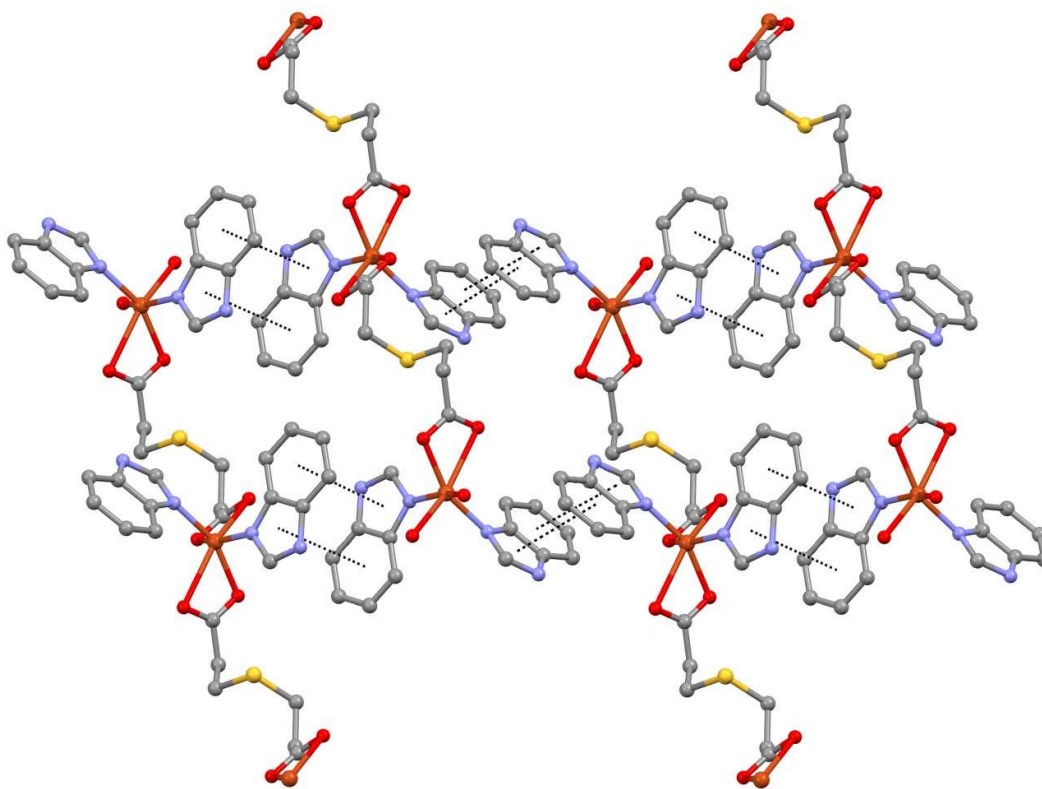


**Fig. 4.** The  $\pi \cdots \pi$  interactions for **2**

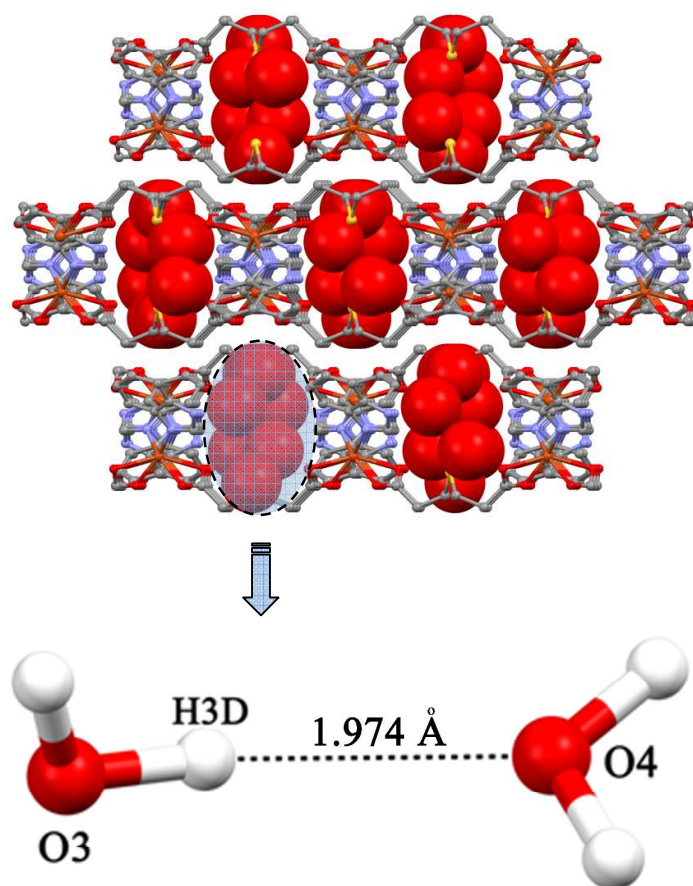


**Fig. 5.** 3D supramolecular network of **2** which has D2 water cluster inside the voids

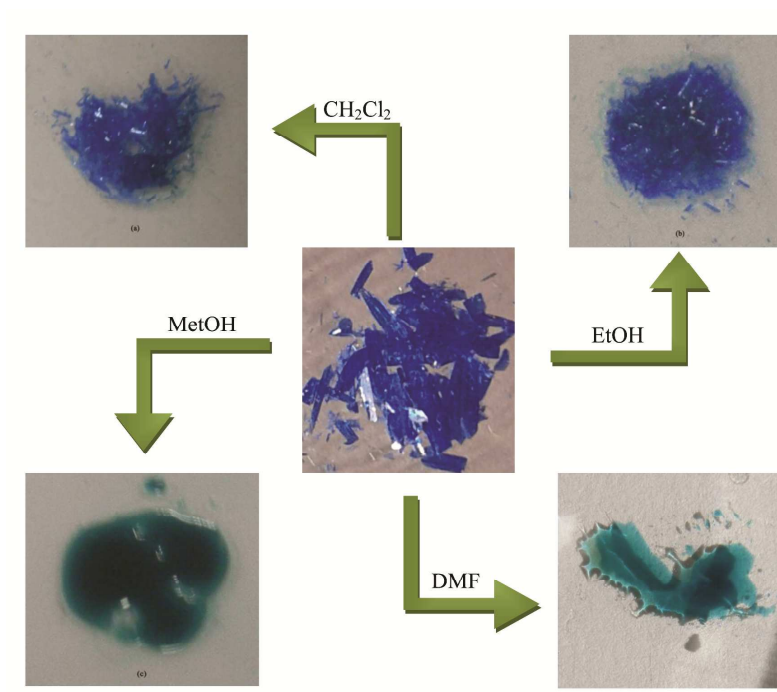


**Fig. 6.** The color change photographs of complex **1** in methanol, ethanol, dichloromethane, dimethylformamide

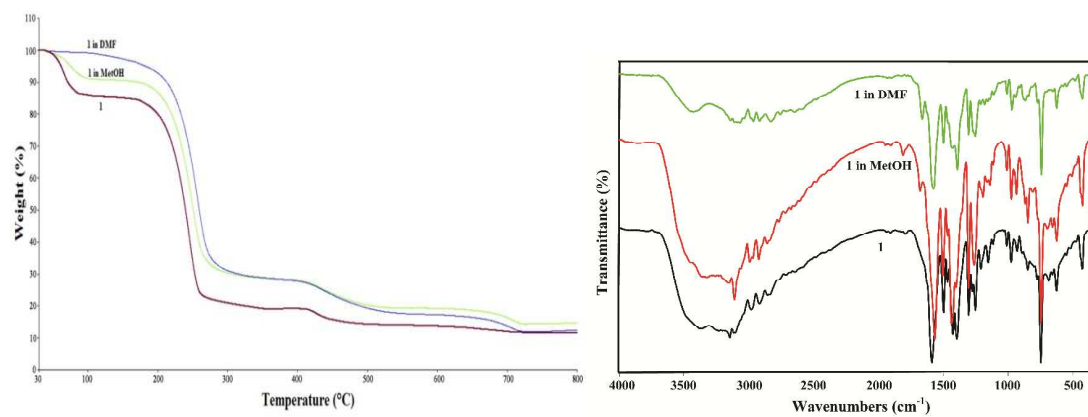


**Fig. 7.** TG curves (a) and IR spectra (b) of complex **1**, **1@MetOH** and **1@DMF**.



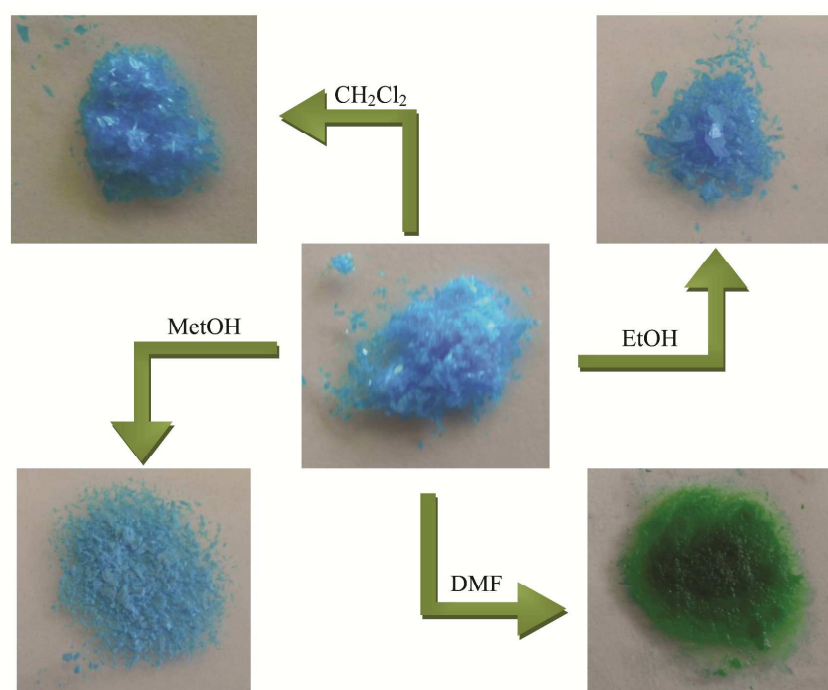


**Fig. 8.** The color change photographs of complex 2 in methanol, ethanol, dichloromethane, dimethylformamide

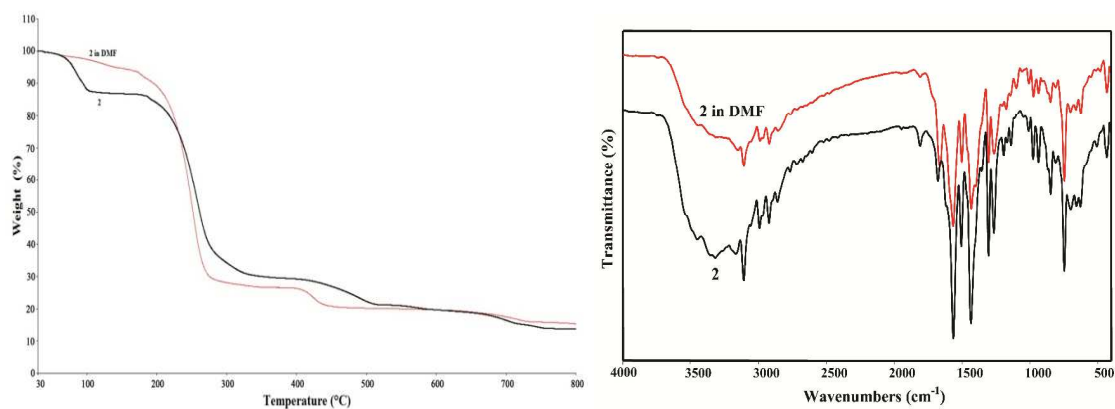


**Fig. 9.** TG curves and IR spectra of complex **2** and **2@DMF**

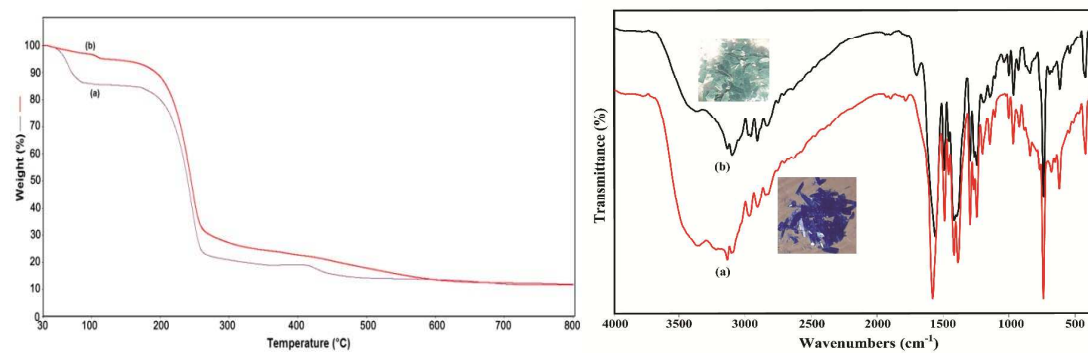


**Fig. 10.** TG curves and IR spectra of (a) as-synthesized complex **1** (b) complex **1** after heating at 65°C

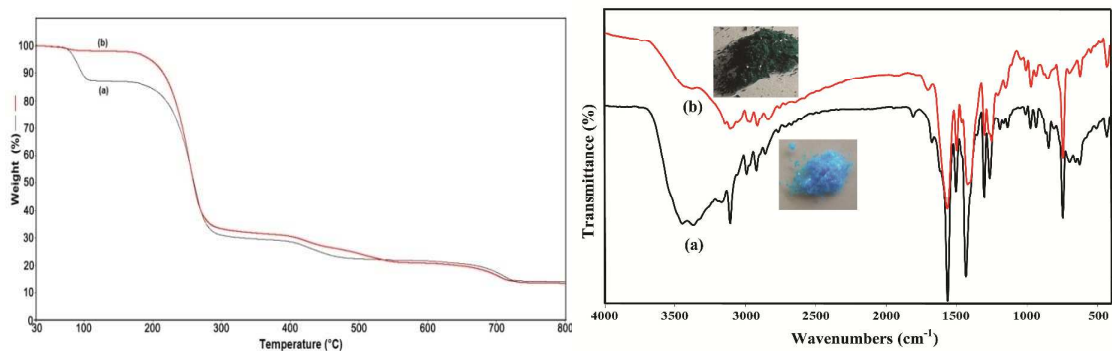


**Fig. 11.** TG curves and IR spectra of (a) as-synthesized complex **2** (b) complex **2** after heating at 65°C

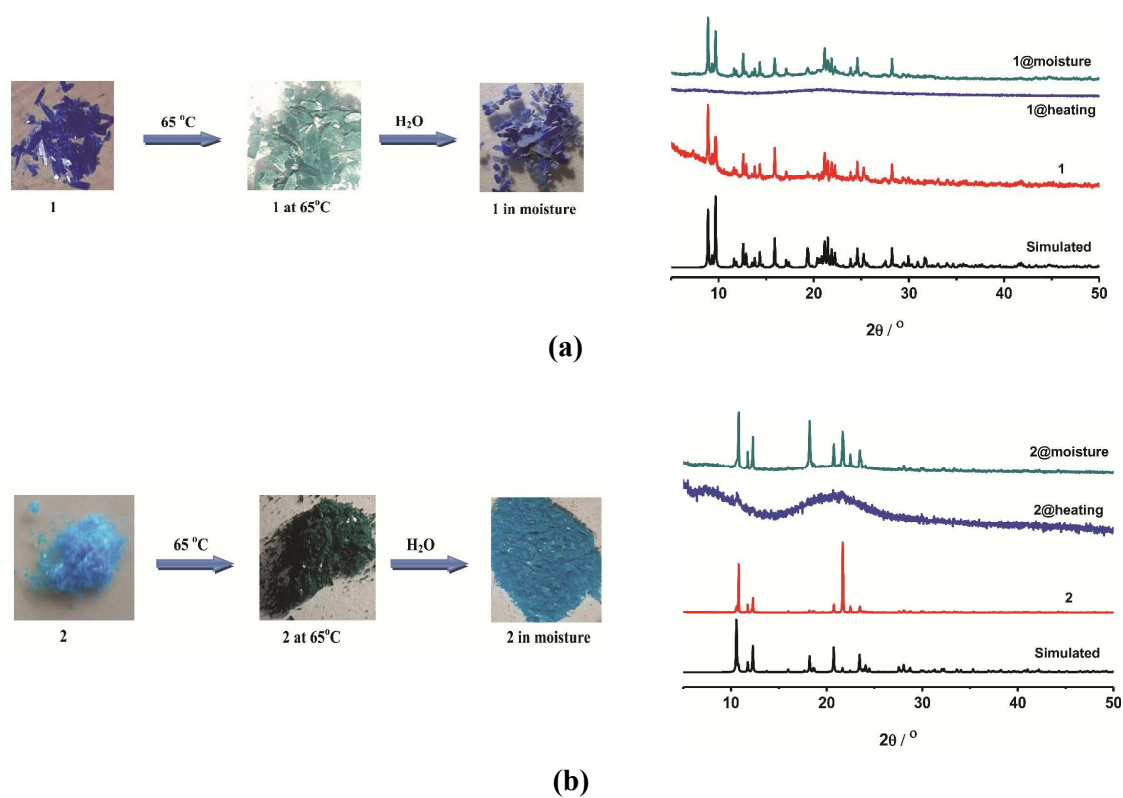


**Fig. 12.** The pictures and PXRD patterns of complexes **1** (a) and **2** (b) showing color changes based on dehydration and rehydration

Two novel coordination complexes were synthesized and characterized. Solvent sensing and thermochromic properties were studied. Complex **1** can be used as a naked-eye sensor for methanol. Complex **2** may be used DMF sensor. Thermochromic behaviors of complexes **1** and **2** were investigated.

